sciendo

ANNALS OF WEST UNIVERSITY OF TIMISOARA PHYSICS

Vol. LXVI, 2024

DOI: 10.2478/awutp-2024-0012

I-MASnBr$_3$ /CZTGS HETEROJUNCTION SOLAR CELL LAYER OPTIMIZATION INVESTIGATED USING SCAPS-1D SOFTWARE EXHIBITED EXCELLENT PERFORMANCE AT 50 %

M. Ghaleb[1,2,*], A. Arrar[1,2,*], A. Hadji Chikh [1,2], H. Bendjilali[3], O. Zerrouki[1]

[1] *Faculty of Technology, University of Relizane, Bourmadia, BP 48000, W. Relizane, Algeria.*
[2] *Laboratory of Physics Thin Layer & Advanced Technologies, University of Relizane, Bourmadia, BP 48000, W. Relizane, Algeria*
[3] *Condensed Matter and Sustainable Development Laboratory (LMCDD), University of Sidi Bel-Abbes, Sidi Bel-Abbes 22000, Algeria*
** Corresponding authors amina.arrar@univ-relizane.dz and mohamed.ghaleb@univ-relizane.dz*
Tel. +213799035690

Article Info

Received: 05.03.2024
Accepted: 04.06.2024

Keywords:
heterojunction perovskite, SCAPS-1D, CZTGS, i-$CH_3NH_3SnBr_3$.

Abstract

This paper reports a novel prototype of heterojunction solar cells based on semiconductor/perovskite structure using the solar cell capacitance one-dimensional simulator (SCAPS 1D). The device schematic consists of Glass/ITO/ETL/MASnBr$_3$ /CZTGS/HTL layers with perovskite i-MASnBr$_3$ as the permeable layer. The thickness of the absorber layer, carrier charge concentration, and the effect of temperature and series resistances are optimized. The research examines several critical parameters essential for solar cell performance, including a power conversion efficiency PCE of 50%, an open-circuit voltage V_{oc} of 1.62 V, a fill factor FF of 91.5%, and a short-circuit current density J_{sc} of -34.06 mA/ cm^2. The temperature and series resistance effects, as well as quantum efficiency QE, and J-V curve simulations with varying acceptor density, are investigated.

1. Introduction

Improved solar technology has advanced significantly in recent years, exhibiting a variety of groundbreaking photovoltaic (PV) cell developments. These next-generation panels have various designs and improvements intended to improve overall dependability, minimize degradation, and increase efficiency. Nowadays, the most popular PV solar cell has given rise to several approaches, including PERC (Passivated Emitter Rear Cells) and HJT

(Heterojunction Cells). HJT solar cells employ a standard set of chemicals called layers that limit recombination at the N-P junction, increasing cell efficiency and decreasing losses.

In 2019, the National Renewable Energy Laboratory (NREL) in Golden, Colorado, USA achieved a groundbreaking milestone in solar cell efficiency, setting a world record of 39.5% under sun global illumination. This feat was accomplished through the development of multi-junction concentrator solar cells, signifying a significant leap forward in harnessing solar energy [1,2]. Each of [3,4] also achieved an efficiency exceeding 31% by studying binary perovskites. Therefore, our work is based on studying the structure $MASnBr_3$/CZTGS. We have proposed using (Cu_2BaSnS_4) as a layer for transporting holes, which is a quaternary chalcogenide compound that possesses several desirable properties for efficient hole transportation. Its unique crystal structure and band alignment make it suitable for facilitating the movement of positively charged carriers (holes) within the device [5]. By incorporating CBTS as a hole transport layer, it has the potential to minimize charge recombination losses and improve the overall device efficiency. Additionally, CBTS has a rather large bandgap Eg=1.9eV [6].

The absorbent layer CZTGS, resulting from the addition of Germanium Ge for the famous compound CZTS (Copper Tin Sulfide) is currently attracting a lot of attention from the scientific community. CZTGS (Copper Tin Germanium Sulfide) possesses a tunable band gap that can be adjusted by controlling the Ge content easily ([Ge]/[Sn] + [Ge]). This property reduces scarce and toxic components including Ga, Se, and Pb, making CZTGS a potential candidate for the top SC of a tandem device [7]. In another way, doping CZTGS with lower amounts of Ge atoms should strengthen the “SS” and “SP” repulsion levels between Ge and S/Se atoms, resulting in a stronger anti-bonding nature of the conduction band minimum (CBM) and enhancing the band gap energy (Eg) value of the CZTGS semiconductor [8,9]. Ford, Chen et al.'s research indicates that CZTGS achieves a remarkable 6.8% efficiency with a J_{sc} value of 21.5, and an Eg of 1.6eV for 70% germanium content. This particular energy band gap is almost exactly in line with what is needed for top-cell applications, it can also be controlled in the band gaps of CZTGS(e) between 1.07eV and 2.0eV by carefully controlling the Ge [10,11]. Additionally, CZTGS is composed of abundant and low-cost elements, making it a cost-effective alternative to other thin-film solar cell materials that may rely on rare or expensive elements [12].

Then comes $CH_3NH_3SnBr_3$, a type of perovskite compound with the chemical formula ABX_3, where A is the organic cation methylammonium (CH_3NH_3+), B is the metal tin (Sn), and X is the halogen bromine (Br). The stability of $MASnBr_3$ needs further investigation to

fully understand how it behaves under different environmental conditions.[13]. $MASnBr_3$ has an estimated bandgap of 1.3eV, indicating its ability to absorb light in the visible to ultraviolet wavelength range. This feature makes it highly appealing for use in photovoltaic devices such as solar cells. Due to its bandgap value, it can efficiently catch photons from sunshine and convert them to electricity [14, 15].

Given the promising properties of $CH_3NH_3SnBr_3$, ongoing research in the field of perovskite materials aims to optimize their stability and performance, which could lead to their integration into various optoelectronic devices, including solar cells [16].

Finally, Titanium dioxide, or TiO_2, is widely used as the electron transport layer that collects and moves photogenerated electrons from the perovskite layer to the electrode (ETL) in a range of solar cell types, including dye-sensitized solar cells (DSSCs) and perovskite solar cells. TiO_2 is a wide-band gap semiconductor, due to the large energy differential (Eg =3.26eV) between its valence and conduction bands, perovskite solar cells can absorb high-energy photons from the solar spectrum. It provides a favorable energy level alignment for efficient charge extraction and aids in preventing electron-hole pair recombination [17]. Due to its unique qualities and ability to work well with other materials, TiO_2 is a popular and effective component in perovskite and dye-sensitized solar cells [18-20].

ITO (indium tin oxide) is a transparent conducting oxide that has been used in solar cells and other optoelectronic devices. It is transparent to visible light, making it suitable for use in transparent solar cells or other optoelectronic devices. Additionally, ITO is a good conductor of electricity, which makes it useful for collecting current in solar cells. It is also stable and not affected by moisture [21]. The work by Ghaleb et al. utilized SCAPS software to investigate how the thickness, the defect density, and doping affect the heterojunction solar cell device output of TiO_2/i-$CH_3NH_3SnBr_3$/$CsPbI_3$/Al (BSF) that achieves a V_{oc} = 1.21V, J_{sc} = 35.63mA/cm^2, FF = 89.84% and PCE =38.98% [22].

In this article, we study and explore the efficiency of a perovskite based, organic, lead-free, glass solar cell /ITO/ETL-TiO_2/i-$CH_3NH_3SnBr_3$/p-$Cu_2ZnSnGeS_4$/HTL-Cu_2BaSnS_4. Our research also delves into various aspects, such as temperature dependence, quantum efficiency (QE), open-circuit voltage, fill factor, short-circuit current density, and the simulation of J-V curves for solar cells with varying Na, Nt, defect density, and series resistances. We provide valuable insights into the design and optimization of PSC structures, contributing to the development of cost-effective and sustainable solar energy systems.

2. Materials and Method

The proposed heterojunction used in this study is Glass/ITO/ETL/i-$MASnBr_3$/p-CZTGS/HTL. The schematic structure and energy band diagram of this work are given below in Fig. 1.

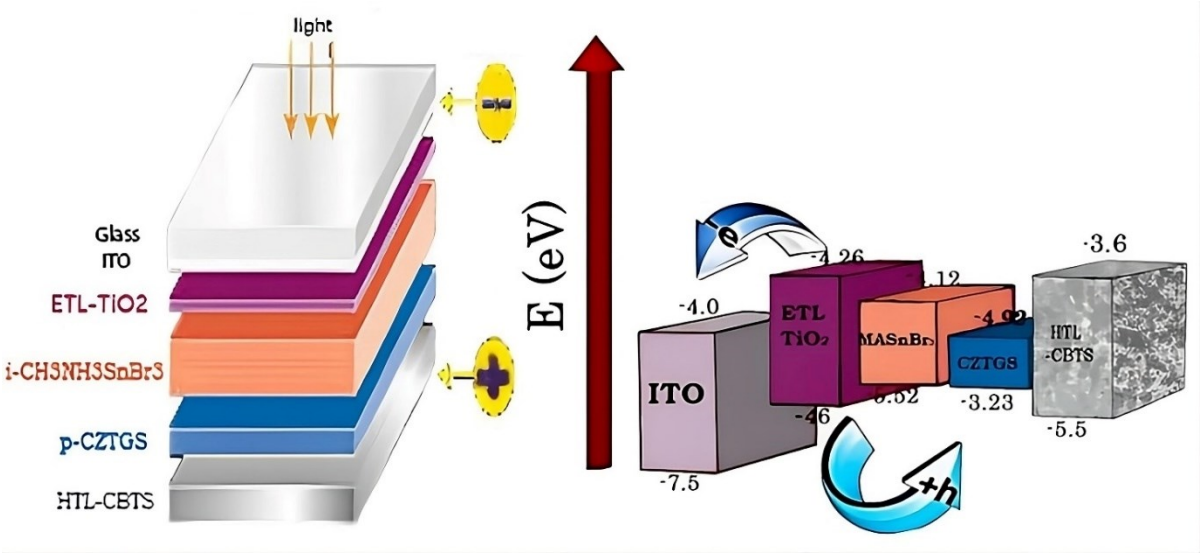


Figure 1. Suggested schematic diagram and energy band diagram of CZTGS/$MASnBr_3$ solar cell

Burgelman from the University of Gent, Belgium, developed the SCAPS-1D (Solar Cell Capacitance Simulator) software in order to identify the numerical simulation of thin-film solar cells [23]. The electrical and optical characteristics of several types of solar cells, including perovskite solar cells, are modelled and evaluated using a one-dimensional modelling approach. This method simplifies the modelling process by assuming that the parameters of the solar cell are uniform in one direction. To accurately predict the performance of solar cells under different operating conditions, SCAPS-1D considers several physical processes such as carrier transport, generation, recombination, and optical absorption [24,25].

Various characteristics and situations were considered in the modelling of the photovoltaic cell under illumination. The simulation utilized an electron and hole thermal velocity of 1×10^7 cm/s. This measure denotes the main velocity of charge carriers (electrons and holes) caused by thermal energy at a specific temperature.

The solar cell's Electron Transport Layer (ETL) had a fixed value of 0.05µm. Similarly, the ITO thickness was fixed at 0.4µm, and the Hole Transport Layer (HTL) thickness was determined to be 0.05µm. Our simulations employ the AM 1.5G standard photovoltaic radiation spectrum, which faithfully reproduces the sun spectrum observed on Earth. The power density of this spectrum remains constant at 1000 W/m^2 despite the measured temperature being 300 K. With regards surface recombination velocity of electron and hole the

values are taken constant and equal to 1×10^{7} (cm/s) for each right contact (front) and left contact (back).

All essential simulation parameters have been consolidated and presented in Tables 1. Table 1 regroup the physical parameters employed in our simulation.

Table 1. Input parameters for the simulation of $MASnBr_3$/CZTGS solar cell

	HTL-CBTS	**CZTGS**	**$MASnBr_3$**	**ETL-TiO_2**	**ITO**
Layer thickness (µm)	0.05	Varied	Varied	0.05	0.4
Dielectric constant dk	5.4	10	10	10	3.5
Band gap Eg (eV)	1.9	1.59	1.3	3.26	4
Electron affinity chi (eV)	3.6	4.19	4.17	4.2	9
Effective conduction band density (cm^{-3})	2.2×10^{18}	$2{,}2\times10^{18}$	2.2×10^{18}	1×10^{21}	2.2×10^{18}
Effective valence band density (cm^{-3})	1.8×10^{19}	$1{,}8\times10^{19}$	1.8×10^{18}	2×10^{20}	1.8×10^{19}
Electron mobility ($cm^2V^{-1}s^{-1}$)	30	60	1.6	20	20
Hole mobility ($cm^2\ V^{-1}\ s^{-1}$)	10	20	1.6	10	10
Shallow uniform donor density Nd (cm^{-3})	-	10	1×10^{13}	5×10^{19}	1×10^{21}
Shallow uniform acceptor density Na (cm^{-3})	1×10^{18}	7×10^{16}	1×10^{13}	-	-
Defect density cm^{-3}	1×10^{15}	Varie	Varie	1×10^{15}	1×10^{15}
References	[26,27]	[28,29]	[30]	[31]	[32-34]

3. Results and discussion

3.1. Tuning Layer Thickness for Improved Solar Cell Efficiency: “perovskite and S-C"

Each material's structure in a solar cell has an optimal thickness that allows for maximum light absorption and efficient charge transfer, resulting in the largest profit. Our initial target is to determine the optimal thickness for the perovskite layer $MASnBr_3$ and the semiconductor layer CZTGS. This range varies from 0.1µm to 1.1µm. Additionally, we have set the thickness of the ITO, ETL, and HTL layers at 0.4µm, 0.05µm, and 0.05µm, respectively.

Fig.2 shows the relationship between $MASnBr_3$ and CZTGS layer thickness and solar cell performance. Notably, the greater the thickness of $MASnBr_3$ the better the efficiency (Fig. 2(a)), which rises from 33.36% to 46,8% (Fig. 2(a)).

Furthermore, the reported fill factor (FF) of 88% indicates that the solar cells are capable of efficiently utilizing the available power from the incident light. A high FF is desirable as it reflects the ability of the solar cells to minimize losses and maximize power output [35].

The J_{sc} value of 34.89mA/cm^2 is also significant. The short-circuit current represents the amount of current produced by the solar cells when they are connected in a short-circuit configuration, indicating their ability to create a significant current. This attribute is beneficial for applications that necessitate a substantial current output, such as in power-intensive devices or systems [36].

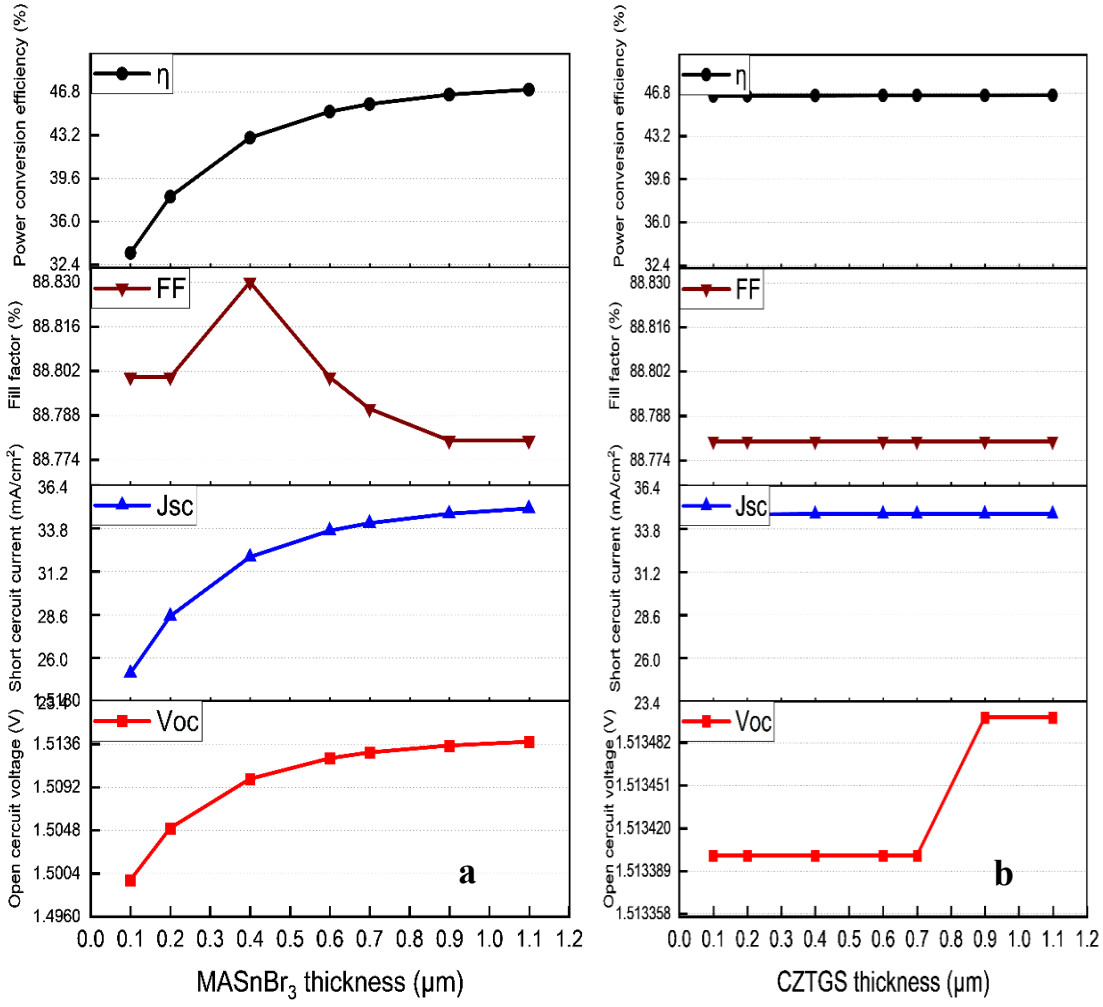


Figure 2. The influence of (a) MLASnBr$_3$ and (b)CZTGS layer thickness on the properties of solar cell

Lastly, the open circuit voltage (V_{oc}) corresponds to the maximum voltage that can be achieved across the solar cell terminals when there is no external load. The reported value of 1.5 volt is rather high compared to conventional cells.

This observation suggests that the thickness of the MASnBr$_3$ plays a significant role in enhancing the performance of the solar cells. This finding underscores the importance of

optimizing the layer thickness during the fabrication process to achieve higher efficiencies in solar cell design.

As demonstrated in Fig. 2(b), the solar cell parameters only marginally improved after changing the thickness of CZTGS therefore the CZTGS layer's thickness had little impact.

Fig. 3(a) demonstrates the impact of layer thickness on the J-V (current-voltage) curves. The specific layer being referred to here is the $MASnBr_3$ layer, and its thickness is varied from 1µm to 1.1µm. The J-V curve represents the relationship between the current density (J) and the voltage (V) across a device. We can conclude that an increase in J_{sc} from 22mA/cm^2 to 34mA/cm^2 suggests that a thicker $MASnBr_3$ layer allows the solar cell to generate higher current densities under illumination. This indicates that a thicker $MASnBr_3$ layer is capturing and transporting more charge carriers (electrons and holes), when exposed to light. The curves also indicate that the thickness of the $MASnBr_3$ layer plays a significant role in determining the device's performance. Thicker layers appear to enhance the efficiency of the solar cell, leading to higher J_{sc} values.

Fig. 3(b) illustrates the high quantum efficiency observed in the solar cell, particularly in the visible range of light. With the change of thickness, this implies an increase in thickness allows perovskite composition to absorb light more efficiently, which is roughly 100% in thickness 1,1µm.

Following these enhancements, we will take the thickness of $MASnBr_3$ and CZTGS to 0.9µm and 0.3µm, respectively, for use in the remainder of the study.

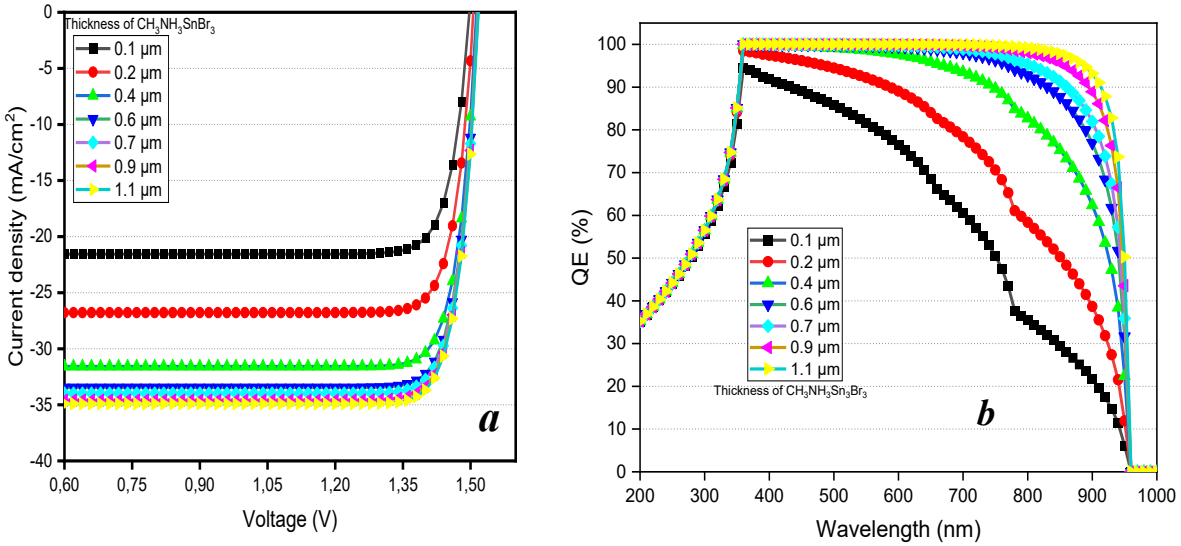


Figure 3. Layers thicknesses effects on the J-V and QE curves

3.2. Effect of CZTGS carrier concentration on solar cell performance

The analysis presented in Fig. 4 explores the impact of acceptor density (CZTGS) on various characteristics of a solar cell, covering a range from $7\times10^{15}cm^{-3}$ to $7\times10^{21}cm^{-3}$. The study focuses on efficiency, fill factor, short-circuit current density, voltage, and quantum efficiency.

The most significant result in this part is the extraordinary improvement in efficiency (PCE) as the acceptor density is increased. At the highest tested acceptor density of $7\times10^{21}cm^{-3}$, the efficiency reaches an impressive 50% (Fig. 4(a)). The fill factor also experiences an extraordinary improvement and reaches about 91% at the highest acceptor density. This indicates better charge carrier collection and reduced losses, leading to a highly efficient use of photogenerated current in the solar cell. Surprisingly, the short-circuit current density remains relatively constant throughout the investigated range of acceptor densities (Fig. 4(b)). This suggests that changes in acceptor density have a limited impact on the amount of current generated under short-circuit conditions, and the solar cell maintains a consistent current output of around $34mA/cm^2$. The open-circuit voltage experiences a moderate increase when increasing acceptor density. Starting from 1.51V at the lowest density, it reaches 1.62V at the highest density tested ($7\times10^{21}\ cm^{-3}$).

It appears that the quantum efficiency (QE) of the solar cell remains unaffected by changes in the acceptor density (CZTGS) (Fig. 4(c)). However, the quantum efficiency exhibits consistently high values across the entire visible spectrum, ranging from 0.2μm to 1μm.

The acceptor's density variations in the investigated range from $1\times10^{15}cm^{-3}$ to $1\times10^{21}cm^{-3}$ do not significantly impact the quantum efficiency of the solar cell.

This means that regardless of the acceptor's density within the studied range, the solar cell's ability to convert incident photons in the visible spectrum into charge carriers (electrons or holes) remains stable and high. This means that other factors, such as material properties, interfaces, and device architecture, play a more significant role in influencing quantum efficiency compared to the acceptor's density in the tested range.

On the other hand, the findings demonstrate that higher acceptor densities in the tested range lead to a more efficient solar cell design, resulting in unprecedented levels of efficiency (50%) and fill factor (91%). These results are significant and could have practical implications for the development of highly efficient solar cells.

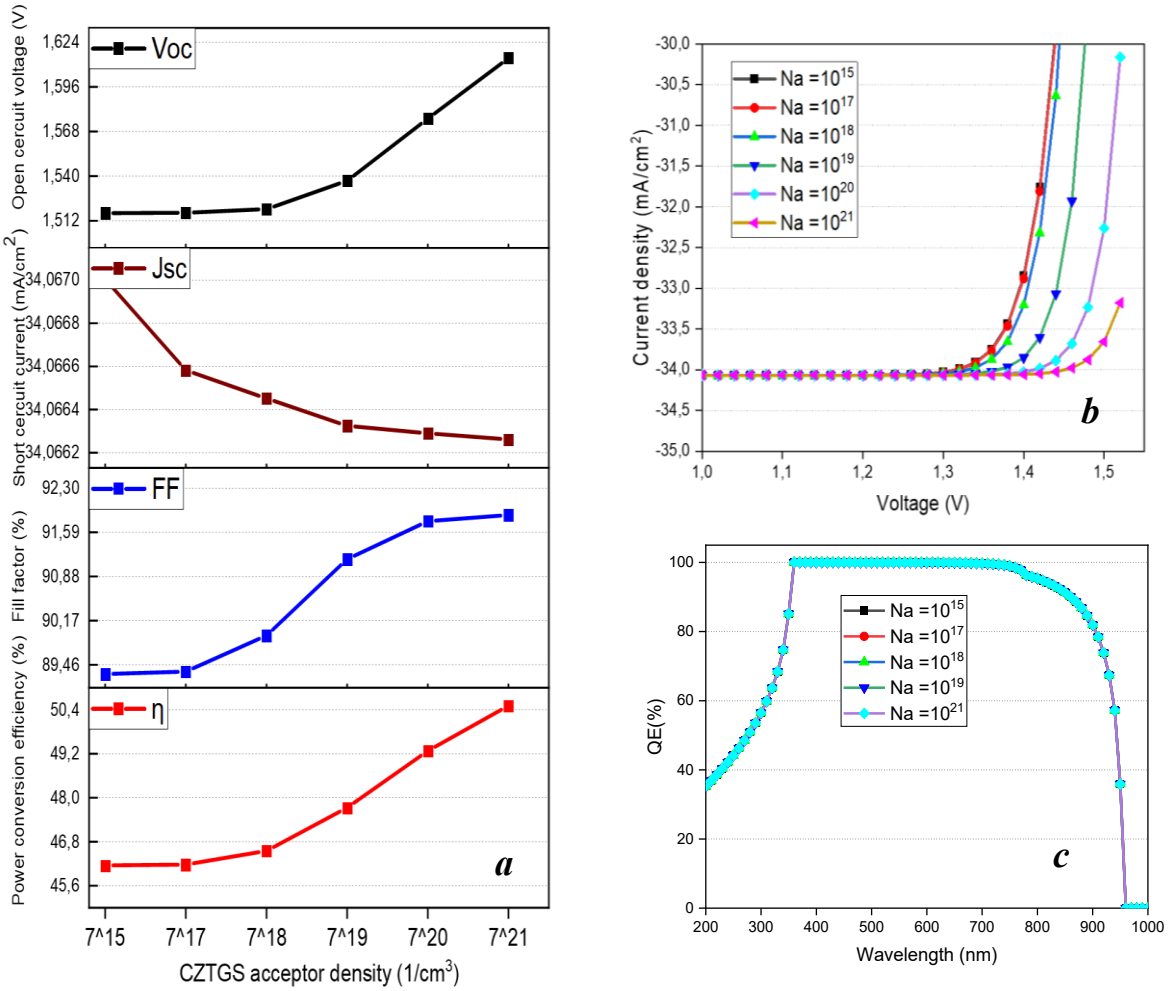


Figure 4. Effects of acceptor density on photovoltaic parameters

3.3. Impact of temperature and series resistances on $MASnBr_3$/CZTGS

We will now examine the impact of temperature and series resistance on the devices. Specifically, we will vary the temperature within the range of 270k to 370k. The resistance of the chain will be raised from 1Ω.cm^2 to 5Ω.cm^2.

Table 3. The effect of temperature changes on $MASnBr_3$/CZTGS

Temperature (K)	PCE η	FF	J_{sc}	V_{oc}
270	48.72	89.18	34.065762	1.6036
290	46.96	89.21	34.066267	1.5450
310	45.37	89.39	34.067029	1.4901
330	43.86	89.29	34.067715	1.4418
350	42.35	88.97	34.068543	1.3974
370	40.88	88.50	34.069391	1.3557

As the temperature increases from 270K to 370K (Table 3), the parameters of the solar cell are negatively affected. This is in line with the general behaviour of solar cells, as higher temperatures can lead to decreased efficiency and performance. At 270K (lower temperature), the solar cell exhibits higher parameter values: Efficiency (PCE): 48%, Fill Factor (FF): 89.18%, Short-Circuit Current Density (J_{sc}): 34.05mA/cm^2, Open-Circuit Voltage (V_{oc}): 1.6V. As the temperature increases to 370K, the parameter values decrease; Efficiency (PCE): decreases to 40%, Fill Factor (FF): decreases to 88.5%, Short-Circuit Current Density (J_{sc}): Remains constant at 34.05mA/cm^2, Open-Circuit Voltage (V_{oc}): decreased to 1.35V.

The findings suggest that elevated temperatures have a detrimental effect on the operation of the solar cell, resulting in decreased efficiency and fill factor. The short-circuit current density (J_{sc}) remains consistent across the temperature range under investigation.

The temperature sensitivity of solar cells is well-known in the field, and this behaviour is often taken into account when designing and modelling solar cell systems. Elevated temperatures can increase the rate of recombination, reduce carrier mobility, and affect the thermal generation of electron-hole pairs, all of which contribute to performance degradation [37,38].

Table 4. The effect of Series Resistances changes on $MASnBr_3$/CZTGS.

Resistance (Ω.cm^2)	**PCE (η)**	**FF**	**J_{sc}**	**V_{oc}**
1	45.03	87.14	34.066611	1.5169
2	43.92	84.98	34.066611	1.5170
3	42.81	82.84	34.066611	1.5171
4	41.71	80.71	34.066611	1.5171
5	40.63	78.61	34.066611	1.5171

In Table 4, for each increase of 1Ω cm^2 in series resistance, there is a 1.1% decrease in efficiency. This means that as the series resistance increases from 1Ω.cm^2 to 5Ω.cm^2, the overall efficiency of the solar cell decreases. This deterioration rate is good compared to traditional cells. For every additional Ohm.cm^2 of series resistance, there is a deterioration in the fill factor by 2.13%. This indicates that increasing series resistance has a negative impact on the solar cell's ability to utilize the available photogenerated current, leading to a decrease in the fill factor. The table shows that the short-circuit current density (J_{sc}) and open-circuit voltage (V_{oc}) are not affected by changes in the series resistance. Both J_{sc} and V_{oc} remain constant, whether the series resistance is 1 or 5Ω.cm^2.

3.4. Effect of Interface Defect States

In this part, a detailed study was conducted on the impact of defect states at the interfaces of various layers within a solar cell structure: ETL/$MASnBr_3$, $MASnBr_3$/CZTGS, CZTGS/HTL. Defect states can have a significant influence on the performance of solar cells, as they can trap charge carriers (electrons and holes), affect charge transport, and ultimately impact the overall efficiency of the device [39, 40]. Table 5 shows the parameters used in the simulation.

Table 5. Optimized parameters

Parameters	**Value**
defect type	Neutral
capture cross-section electrons (cm^2)	1×10^{-19}
capture cross-section holes (cm^2)	1×10^{-19}
energetic distribution	Single
reference for defect energy level Et	Above the highest EV
Energy concerning Reference (eV)	0.6

At the ETL/perovskite interface, the density of defect states varies from 1×10^{10} cm^{-2} to 1×10^{20} cm^{-2}. It has been noted that V_{oc} and efficiency decrease sharply (Fig. 5(a)) from 1.43V to 0.92V, and 42.54% to 23.95%, respectively. However, we did not find a notable observation for J_{sc} and FF, though both decrease (Fig. 5(b)) with the increase of defect state density.

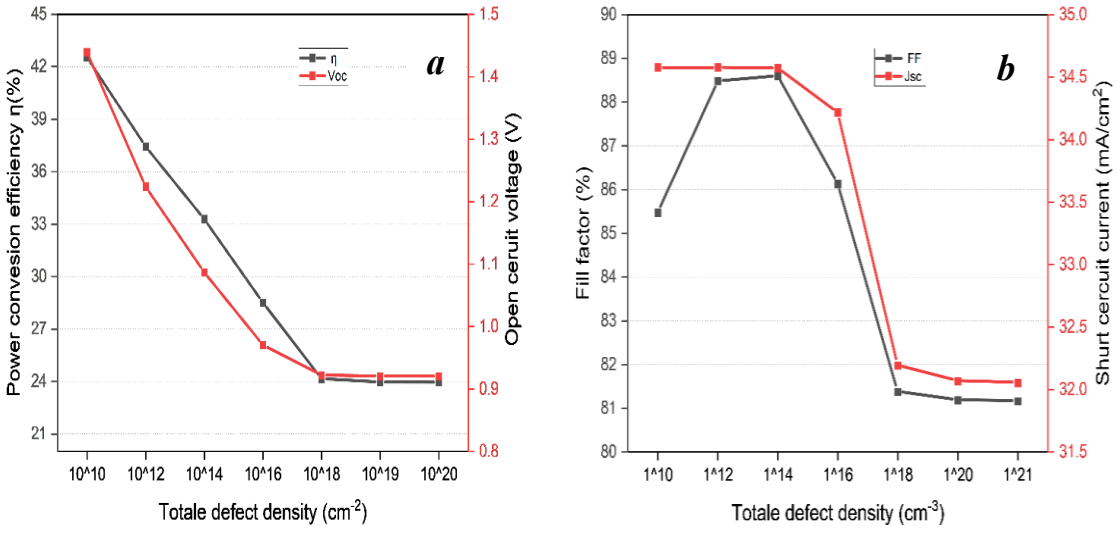


Figure 5. The impacts resulting from changes in defect density (Nt) at the TiO_2/$MASnBr_3$ interface, (a) alterations in efficiency and V_{oc}, and (b) adjustments in J_{sc} and fill factor

It can be observed that increases in the level of defect state mainly impact the open circuit voltage rather than the short circuit current. Therefore, the change in V_{oc} is mainly attributable to the drop in the efficiency of the device. Hence, defect tolerance at $TiO_2/CH_3NH_3SnBr_3$ can be figured up to $1\times10^{16}cm^{-2}$. After that, the solar cell parameters are greatly affected.

On the other hand, at the Perovskite/semiconductor ($MASnBr_3$/CZTGS) interface, the density of defect states varies from 1×10^{10} cm^{-2} to 1×10^{20} cm^{-2}. It has been revealed that V_{oc} and efficiency decrease sharply (Fig. 6(a)) with the increase of defect density at the perovskite/S-C interface. As for the short circuit current, it was not affected by the change in the defect density interface. However, the filling factor fluctuated slightly with changes in the defect density (Fig. 6(b)). This is exemplified by the higher number of recombination centres, often referred to as trap centres, which are responsible for hindering the efficient movement of charge carriers in CZTGS [41].

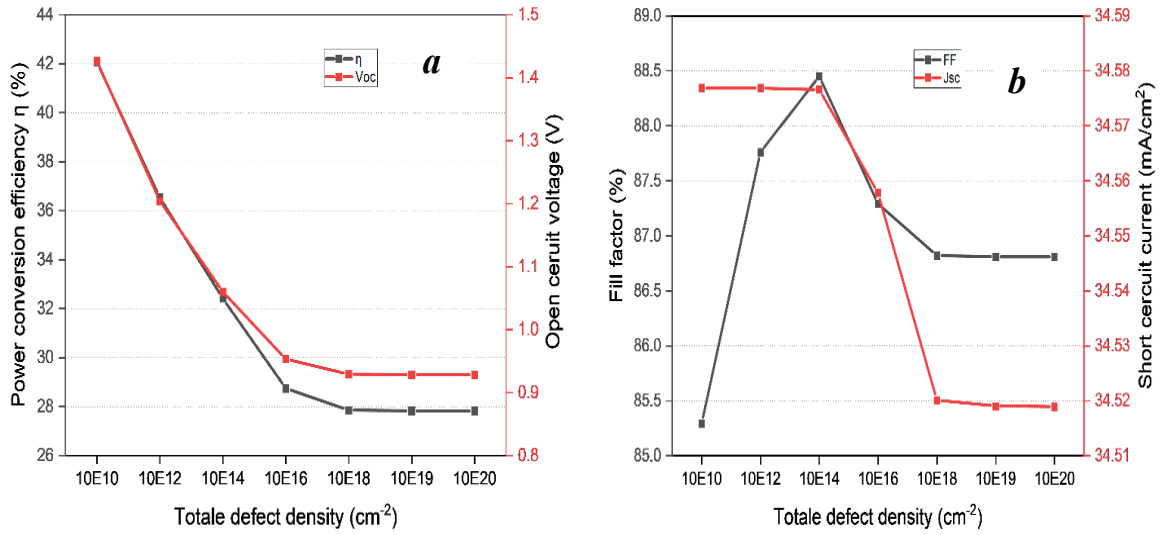


Figure 6. The impacts resulting from changes in defect density (Nt) at the $MASnBr_3$/CZTGS interface, (a) alterations in efficiency and V_{oc}, and (b) adjustments in J_{sc} and fill factor.

The research findings highlight that defect states at the interface between the perovskite and semiconductor significantly affect the efficiency of perovskite solar cells. The decline in open-circuit voltage and efficiency can be ascribed to trap centres, which promote charge carrier recombination and impede effective charge transport. Defects in a material create extra energy levels in the space between the valence and conduction bands. These levels can capture charge carriers, causing them to get stuck and resulting in non-radiative recombination. This hinders the production of photocurrent and the overall efficiency [42].

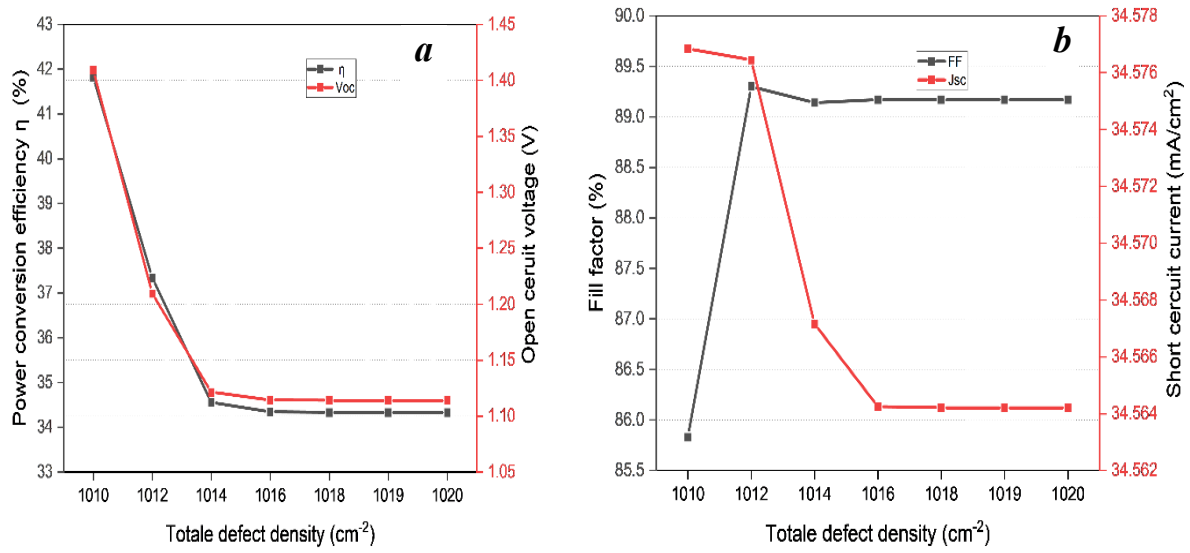


Figure 7. The impacts resulting from changes in defect density (Nt) at the CZTGS/HTL interface, (a) alterations in efficiency and V_{oc}, and (b) adjustments in J_{sc} and fill factor

The last interface that was studied is the interface CZTGS/HTL shown in Fig. 7. Where the value of efficiency and V_{oc} keeps dropping until it reaches a minimum value at the defect density level of $1 \times 10^{14} cm^{-2}$. As we can see, efficiency drops from 42% to 34 %, and the same thing for open-circuit voltage as it drops from 1,41V to 1,1V when we change the defect density from $1 \times 10^{10} cm^{-2}$ to $1 \times 10^{14} cm^{-2}$. The range of different defect interface densities shows a 7% change appears in the PCE (Fig. 7(a)). Regarding the short-circuit current and fill factor, there was no noticeable effect as shown in (Fig. 7(b)). After changing the defect density below $1 \times 10^{14} cm^{-2}$, there are no noticeable output differences in the PCE and the rest of the parameters. It can be achieved that the CZTGS-based material delivers the maximum J_{sc} of $34.091 mA/cm^2$. By observing the results and drawings, we conclude that in the CZTGS/HTL interface, no change was affected compared to the other interfaces that were studied. The stability of other parameters like J_{sc} and FF suggests that the defects mainly influence transport processes rather than light absorption or charge collection. This is probably due to the compatibility between the diode surfaces of the semiconductors CZTGS and CBTS, which plays a crucial role in maintaining the interface's performance stability across different defect densities.

3.5. Effect of $MASnBr_3$ and CZTGS Defect States

Amphoteric native defects are a type of native (or intrinsic) defect in semiconductor materials that can affect their properties. The key feature of amphoteric defects is the concept

of the Fermi level stabilization energy (EFS), which is universally located at about 4.9eV below the vacuum level for all semiconductors [43].

Table 6. The parameters used in the simulation

Parameters	**$MASnBr_3$**	**CZTGS**
defect type	Uniform	Single Donor
capture cross section electrons (cm^2)	1×10^{-19}	2×10^{-14}
capture cross-section holes (cm^2)	1×10^{-19}	2×10^{-14}
energetic distribution	Single	Single
reference for defect energy level Et	Above the highest EV	Above the highest EV
Energy concerning Reference (eV)	0.6	0,6
Defects density Nt (cm^{-3})	Varied [30]	Varied [29]

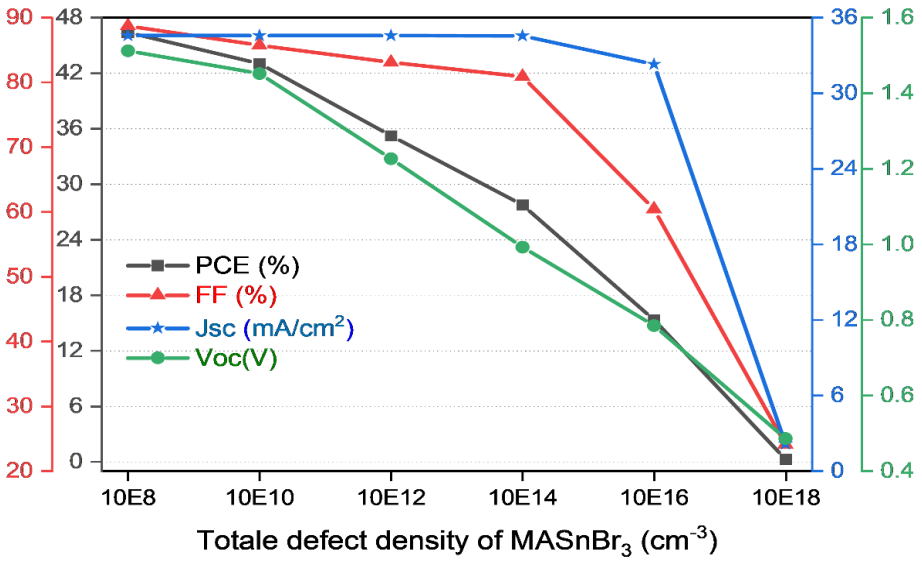


Figure 8. The perovskite's overall defect density effect on a solar cell

The conductivity of $CH_3NH_3SnBr_3$ can be influenced by a variety of factors, including the deposition of Sn and halide molecules, the presence of defects, and the incorporation of other materials. Where the Sn^{2+} cation is very prone to oxidation during the process of fabrication, which is attributed to defects inside the perovskite structure [44,45], In this part, the amphoteric defect has been considered above the Ev of the absorber layer with a uniform energetic distribution where the defect state has been varied from 1×10^{8} cm^{-3} to 1×10^{18} cm^{-3}.

Figure 8 exhibits the influence of amphoteric defect on solar cell parameters. We have found, as shown in Fig. 8, that all parameters of the solar cell are greatly and very much affected by the change in the total defect density of the perovskite layer, as the efficiency decreased from 42% to approximately 1%, and the same for the fill factor, which decreased from 88% to 25%, as well as the short circuit current, decreased from 34mA/cm^2 to 2mA/cm^2 the open circuit voltage decreased from 1.51V to 0.48V. These results indicate the active role played by the perovskite layer in the solar cell device, and both [30,49] found the same results that we found about the $MASnBr_3$ effect. With the increase of defect densities, the unwanted recombination rate increased as the defects created the dangling bonds, which act like the trap state for the photo-generated charge carriers. This is the reason behind the terrible decrease in solar cell parameters [30,49].

Now we analyze and discuss the effect of the CZTGS defect density, which is shown and summarized in Fig. 9. Several experimental studies have shown that the addition of Ge to CZTS materials can enhance device performance, particularly the open circuit voltage (V_{oc}) [47,48], and in various previous experiences Ge incorporation in CZTS material can increase the sizes of the crystalline grains, increase the carrier lifetime, and decrease the band-tail energy, which can improve the performance of solar cells [49]. It also improves their performance by minimizing interface defects and reducing the likelihood of Sn-S secondary phase formation.

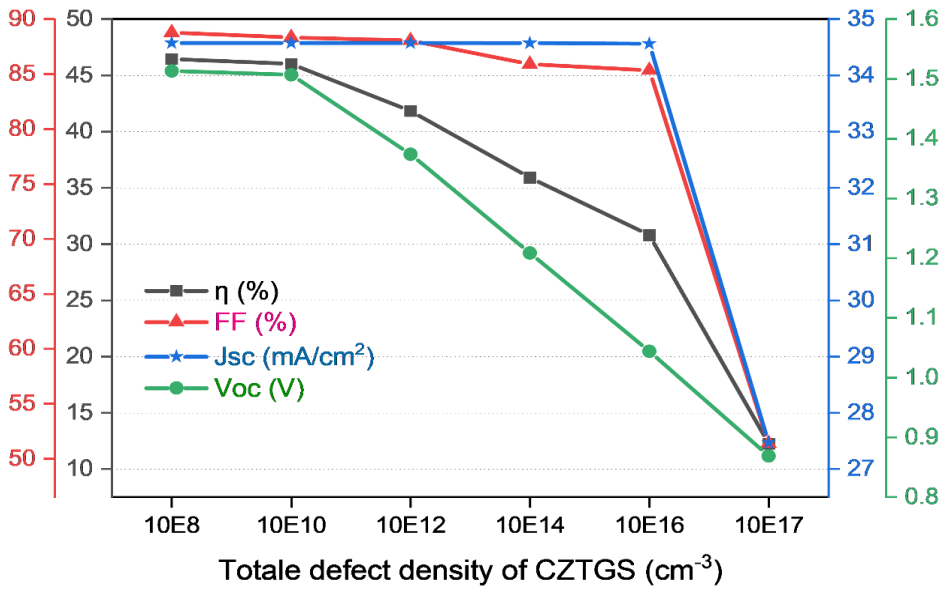


Figure 9. The CZTGS overall defect density effect on a solar cell

It can be noted that the defect density of the CZTGS layer did not significantly affect the cell performance compared to the previous perovskite layer, only the efficiency decreased from 46% to 30% in the range of defect density 1×10^{8} to $1 \times 10^{17} cm^{-3}$, as well as for the open circuit voltage from 1,53V to 1,05V, after which it decreased very clearly. As for the fill factor and the short circuit current, it was not affected in this area, and this confirms the Germanium integration experiments [41,29].

These defects can be mitigated through robust quality control measures during the production and installation of solar panels to minimize the occurrence of defects [50]. Regular maintenance and inspection of solar panels to identify and address any defects or performance issues [51]. Developing materials and methodologies to reduce the defect density in solar cells, such as crystal growth techniques, post-treatments, and interfacial modifications [52].

3.6. Comparison of SCAPS-1D Results with simulation Work

A comparison of the results we obtained with recent theoretical and experimental research with different configurations devices is given in Table 7. In comparison with all of the previous simulation results, all of the studied device performances were significant, and we have revealed the maximum PCE of 30- 44%, which could aid in the identification of future configurations that are more efficient.

Table 7. A comparison of the simulation results

Device Structure	Open Circuit Voltage (V)	Short Circuit Current (mA/cm^2)	Fill Factor (%)	Efficiency (%)	Reference
FTO/ZnO/ $CH_3NH_3SnI_3$/CZTS/Pt	1.03	34.32	86.39	30.42	[53]
TCO/TiO2/$CH_3NH_3PbI_3$/CuI /Pt	1.1169	33.60	89.03	33.41	[54]
FTO//$CsSnGeI_3$/Cu_2O/Au	1.22	28.19	89.53	31	[55]
Triple-junction (GaInP/GaAs/Si)	1.1	29	87.0	35.9	[56]
FTO/ETL/$CsGeI_2Br$/$CsGeI_3$/ HTL/Metal	1.14	32	90	33	[57]
ZnSe/$CuSbSe_2$/CGS	0.9345	58.943	79.46	43.77	[58]
$FASnI_3$/$CH_3NH_3SnI_3$/$FASnI_3$	1.23	33.43	88.64	35.73	[59]

3.7. Comparison of SCAPS-1D results with experimental work

In Table 8, the comparison of numerical simulations using Scaps-1d program and experimental results; Through a comparative study between SCAPS-1D simulations and

experimental observations, this comparison confirms the reliability of numerical simulations in one dimension for predicting the behavior of heterojunction devices. The close agreement between simulated and experimental results underscores the utility of SCAPS-1D as a valuable tool for device design, optimization, and performance analysis.

Table 8. A comparison of the simulation and experimental results

Device Structure	A method	Open Circuit Voltage (V)	Short Circuit Current (mA/cm^2)	Fill Factor (%)	Efficiency (%)	Ref
FTO/SnO_2 /$FAPbI_3$ /Spiro-OMeTAD	Exp	1.123	25.58	73,26	21.07	[60]
	Simul	1,122	25,18	74,71	21.07	
Perovskite	Exp	1.09	23.80	75.16	19.41	[61]
	Simul	1.09	23.50	75.55	19.41	
CIGS	Exp	0.72	36.30	76.80	20.10	[61]
	Simul	0.72	36.22	77.05	20.08	
Proof of helping a program achieve better efficiency	Exp	0.47	37.99	78.42	14.01	[62,63]
	Simul					

4. Conclusion

The study effectively examined the impact of different physical factors on the efficiency of a heterojunction solar cell based on $MASnBr_3$/CZTGS. The parameters investigated encompassed the thickness of i-$MASnBr_3$, the thickness of the CZTGS absorber layer, the density of acceptors, temperature, and the impact of series resistance and defect density. Pre-existing research and experimental data were utilized to stabilize the parameters before commencing the device optimization process. This ensured precise simulations and established a dependable starting point for future tests.

The optimization process yielded a remarkable outcome, attaining a 50% efficiency by utilizing particular thicknesses of CZTGS and $MASnBr_3$, along with a specific acceptor density. The efficiency of the solar cell can be further improved by doping the CZTGS layer, which can alter the characteristics of the absorber layer and enhance overall performance. The study also indicated that the $MASnBr_3$/CZTGS-based solar cell performs better in lower-temperature conditions. Furthermore, the investigation revealed that the influence of heightened series resistance on energy conversion is relatively insignificant, implying that the solar cell demonstrates a reduced rate of deterioration. This suggests that the decrease in efficiency caused by the rise in series resistance is negligible compared to the improvements

obtained through other optimizations. By resolving and reducing flaws, solar cells' total efficiency and performance can be enhanced, resulting in more efficient consumption.

The research offers valuable insights into optimizing heterojunction solar cells based on $MASnBr_3$/CZTGS and presents potential solutions for further enhancing their efficiency. Nevertheless, it is crucial to recognize that this study is limited in scope. Additional research and validation are required to comprehensively understand and improve the solar cell design for practical use. Future investigations can utilize these findings to explore other factors and methods, thereby enhancing the design and functionality of heterojunction solar cells based on $MASnBr_3$/CZTGS. Further study in this field has the potential to yield more effective and economically feasible solar cell technologies that can be utilized in renewable energy systems.

Acknowledgment

We are grateful to the University of RELIZANE for supporting this work, which is included in the project of PRFU N° B00L02UN480120220002. Furthermore, the first author gratefully acknowledges Prof. Marc Burgelman, University of Ghent, Belgium for providing the SCAPS 1-D simulation on software

Author Contributions All authors contribute equally to the manuscript.
Funding No funding was received for conducting this study.
Conflict of interest The authors have not relevant financial or non-financial interests to disclose.

References

[1]R. M France, J. F. Geisz, T. Song, W. Olavarria, M. Young, A. Kibbler, A. Steiner. "Triple-junction solar cells with 39.5% terrestrial and 34.2% space efficiency enabled by thick quantum well superlattices". Joule, **6**(5) (2022) 1121–1135. https://doi.org/10.1016/j.joule.2022.04.024

[2]R. R. King, D. C. Law, K. M. Edmondson, C. M. Fetzer, G. S. Kinsey, H. Yoon, R. A. Sherif, and N. H. Karam, Appl Phys Lett. (2007) "40% efficient metamorphic GaInPGaInAsGe multijunction solar cells". Applied Physics Letters **90**(18) (2007) 183516. https://doi.org/10.1063/1.2734507

[3] S. Bhattarai1, M.K.A. Mohammed, J.Madan, R.Pandey, M.Z.Ansari, A.N.Z. Rashed, M.Amamiand, M.K. Hossain, Performance Improvement of Perovskite Solar Cell Design with Double Active Layer to Achieve an Efficiency of over 31%. Sustainability **15** (2023) 13955. https://doi.org/10.3390/su151813955

[4]S. Bhattarai, R. Pandey, J. Madan, S. Tayeng, P. K. Kalita, M. Z. Ansari, L. Ben Farhat, M. Amamif, M.K. Hossain, "Comparative study of distinct halide composites for highly efficient perovskite solar cells using a SCAPS-1D simulator", RSC Adv. **13** (2023) 26851. https://doi.org/10.1039/d3ra04134d

[5]G. Jie, C.R. Grice, Y. Yanfa, "Cu-based quaternary chalcogenide Cu_2BaSnS_4 thin films acting as hole transport layers in inverted perovskite $CH_3NH_3PbI_3$ solar cells & quot" Mater. Chem. A **5** (2017) 2920-2928. http://dx.doi.org/10.1039/C6TA08426E

[6]J. Ge, Y. Yan, "Synthesis and characterization of photoelectrochemical and photovoltaic Cu_2BaSnS_4 thin films and solar cells". Journal of Materials Chemistry C **5**(26) (2017) 6406–6419. https://doi.org/10.1039/c7tc01678f

[7]R. Mannu, S.Padhy, U. P.Singh, "Output parametric optimization of CZTGS bilayer absorber layer: A numerical study". Materials Today: Proceedings **67**(V) (2022) 768-776, https://doi.org/10.1016/j.matpr.2022.07.302

[8]R. Caballero, I. Victorov, R. Serna, J.M. Cano-Torres, C. Maffiotte, E. Garcia-Llamas, J.M. Merino, M. Valakh, I. Bodnar, M. Leo, "Band-gap engineering of $Cu_2ZnSn1xGexS_4$ single crystals and influence of the surface properties". Acta Materialia **79** (2015), 181-187, https://doi.org/10.1016/j.solmat.2015.03.004

[9]M. Singh, T. R. Rana, J.H. Kim, "Fabrication of band gap tuned $Cu_2Zn(Sn_{1-x}Ge_x)(S,Se)_4$ absorber thin film using nanocrystal-based ink in non-toxic solvent". J. of Alloys and Compounds **675** (2016) 370. https://doi.org/10.1016/j.jallcom.2016.03.138

[10]G. M. Ford, Q.Guo, R.Agrawal, H.W Hillhouse, "Earth abundant element $Cu_2Zn(Sn_{1-x}Ge_x)S_4$ nanocrystals for tunable band gap solar cells: 6.8% Efficient device Fabrication". Chem Mater. **23**(10) (2011) 2626. https://doi.org/10.1021/cm2002836

[11] G. Chen, W. Wang, S. Chen, Z. Whang, Z. Huang, B. Zhang, X. Kong, "Bandgap engineering of $Cu_2ZnSn_{1-x}GexS(e)_4$ by adjusting Sn-Ge ratios for almost full solar spectrum absorption". J Alloys Compounds **718** (2017) 236–245. https://doi.org/10.1016/j.jallcom.2017.05.150

[12] R. Scaffidi, G. Birant, G. Brammertz, J. de Wild, D. Flandre, B. Vermang, "Ge-alloyed kesterite thin-film solar cells: previous investigations and current status – a comprehensive review". J. Materials chemistry A **11**(25) (2023) 13174–13194. https://doi.org/10.1039/D3TA01218B.

[13] C. Bernal, K. Yang, "First-principles hybrid functional study of the organic-inorganic perovskites $CH_3NH_3SnBr_3$ and $CH_3NH_3SnI_3$". J. Phys. Chem. C **118**(42) (2014) 24383–24388. https://doi.org/10.1021/jp509358f

[14] S.Bhattarai, P.K. Kalita, I. Hossain, A.S. Alsubaie, K.H. Mahmoud, M.Z. Ansari, P. Janicek, "P.Designing an Efficient Lead-Free Perovskite Solar Cell through a Computational" Method. Crystals **13** (2023) 1175. https://doi.org/10.3390/cryst13081175

[15] S. Bhattarai, R. Pandey, J. Madan, D. Muchahary, D. Gogoi, "A novel graded approach for improving the efficiency of Lead-Free perovskite solar cells". Solar Energy **244** (2022) 255–263.https://doi.org/10.1016/J.SOLENER.2022.08.030

[16] W. Fu, A.G. Ricciardulli, Q.A. Akkerman, R.A. John, M.M. Tavakoli, S. Essig, M.V. Kovalenko, M. Saliba, "Stability of perovskite materials and devices". Materials Today **58** (2022) 275–296., https://doi.org/10.1016/J.MATTOD.2022.06.020

[17] S. Foo , M. Thambidurai, K.P. Senthil, R. Yuvakkumar, Y. Huang, C. Dang. "Recent review on electron transport layers in perovskite solar cells". Int. J. Energy Res. **46**(15) (2022) 21441-21451. https://doi.org/10.1002/er.7958

[18] K. Mahmood, S. Sarwar, M.T Mehran, Current status of electron transport layers in perovskite solar cells: materials and properties. RSC Advances, **7**(28) (2017) 17044–17062. https://doi.org/10.1039/C7RA00002B

[19] B. Tan and Y. Wu, "Dye-Sensitized Solar Cells Based on Anatase TiO_2 Nanoparticle/Nanowire Composites", J. Phys. Chem. B 2006, 110, 32, 15932–15938 https://doi.org/10.1021/jp063972n

[20] B.H. Lee, M.Y. Song, S.Y. Jang, S.M. Jo, S.Y. Kwak, and D.Y. Kim, "Charge Transport Characteristics of High Efficiency Dye-Sensitized Solar Cells Based on Electrospun TiO2 Nanorod Photoelectrodes", *J. Phys. Chem. C* **113**(51) (2009) 21453–21457. https://doi.org/10.1021/jp907855x

[21] Z. Yu, I.R. Perera, T. Daeneke, S. Makuta, Y. Tachibana, J.J. Jasieniak, A. Mishra, P. Bäuerle, L. Spiccia, U. Bach, "Indium tin oxide as a semiconductor material in efficient p-type dye-sensitized solar cells", NPG Asia Materials **8** (2016) e305 https://doi.org/10.1038/am.2016.89

[22] M. Ghaleb, A. Arrar, Z.Touaa, "Optimization and Performance Analysis of a TiO_2/i-$CH_3NH_3SnBr_3$/$CsPbI_3$/Al (BSF) Heterojunction Perovskite Solar Cell for Enhanced Efficiency", *ACS Omega* **8**(40) (2023) 37011-37022. https://doi.org/10.1021/acsomega.3c03891.

[23] M. Burgelman, P. Nollet and S. Degrave, "Modelling polycrystalline semiconductor solar Cells", Thin Solid Films **361-362** (2000) 527-532. https://doi.org/10.1016/S0040-6090(99)00825-1.

[24] B. Z. Bhari, K.S. Rahman, P. Chelvanathan, M.A. Ibrahim, "Numerical Simulation of Ultrathin CdTe Solar Cell by SCAPS-1D". IOP Conf. Ser. Mater. Sci. Eng. **1278**(1) (2023), 012002. https://doi.org/10.1088/1757-899X/1278/1/012002.

[25] N.J. Valeti, K. Prakash, M. K. Singha, "Numerical simulation and optimization of lead free $CH_3NH_3SnI_3$ perovskite solar cell with CuSbS2 as HTL using SCAPS 1D". Results in Optics **12** (2023) 100440. https://doi.org/10.1016/j.rio.2023.100440

[26] M.K. Hossain, M.H.K.Rubel, G.F.I. Toki, I. Alam, Md. F. Rahman, H. Bencherif, "Effect of various electron and hole transport layers on the performance of $CsPbI_3$-based perovskite solar cells". ArXiv :2211.02968. https://doi.org/10.48550/arXiv.2211.02968

[27] Y. H. Khattak, F. Baig, H. Toura, S. Beg, & B. M. Soucase," Efficiency enhancement of Cu2BaSnS4 experimental thin-film solar cell by device modeling". *J.Mat. Scien.* **54**(24) (2019) 14787–14796. https://doi.org/10.1007/S10853-019-03942-6/METRICS

[28] A. D. Adewoyin, M. A. Olopade, O. O. Oyebola, and M. A. Chendo, "Development of CZTGS/CZTS tandem thin film solar cell using SCAPS-1D". Optik, **176** (2019) 132–142. https://doi.org/10.1016/J.IJLEO.2018.09.033

[29] A. A. Abdelkadir, M. Sahal, E. Oublal, N. Kumar, A. Benami, "Performance enhancement investigations of the novel CZTGS thin-film solar cells". Optical Materials, **133** (2022) 112969. https://doi.org/10.1016/j.optmat.2022.112969

[30] Md.I. Samiul, K. Sobayel, A. Al-Kahtani, M.A. Islam, G. Muhammad, N. Amin, Md. Shahiduzzaman, M.Akhtaruzzaman, , "Defect Study and Modelling of SnX_3-Based Perovskite Solar Cells with SCAPS-1D". Nanomaterials **11** (2021) 1218. https://doi.org/10.3390/nano11051218

[31] L.Lin, L.Jiang, P.Li, H.Xiong, Z. Kang, , B. Fan, Y.Qiu, "Simulated development and optimized performance of $CsPbI_3$ based all-inorganic perovskite solar cells". J Solar Energy, **198** (2020) 454-460, https://doi.org/10.1016/J.SOLENER.2020.01.081

[32] M. K.Hossain, M.H.K. Rubel, G.F.I. Toki, I. Alam, M.F. Rahman, H. Bencherif, "Effect of Various Electron and Hole Transport Layers on the Performance of CsPbI3-Based Perovskite Solar Cells": ACS Omega **7**(47) (2022) 43210–43230. https://doi.org/10.1021/acsomega.2c05912.

[33] H.T. Ganem, A.N. Saleh, "Enhancement of the Efficiency of the CZTS/Cds/Zno/ITO Solar Cell By Back Reflection and Buffer Layers Using SCAPS -1D". Iraqi Journal of Science, **62**(4) (2021) 1144-1157. https://doi.org/10.24996/IJS.2021.62.4.11

[34] M.K.Hossain, G.F.I. Toki, I. Alam, R. Pandey, D.P. Samajdar, M.F. Rahman, M.R. Islam, M.H.K. Rubel, H. Bencherif, J. Madan, M.K.A. Mohammed, 'Numerical simulation and

optimization of a CsPbI3-based perovskite solar cell to enhance the power conversion efficiency", New J. Chem., **47** (2023) 4801-4817. https://doi.org/10.1039/D2NJ06206B

[35] A. Abdelkadir, M. Sahal, Theoretical development of the CZTS thin-film solar cell by SCAPS-1D software based on experimental work. Materials Science and Engineering: B **296** (2023) 116710. https://doi.org/10.1016/J.MSEB.2023.116710

[36] U. Saha, A. Biswas, M.K. Alam, "Efficiency enhancement of CZTSe solar cell using CdS(n)/(AgxCu$_{1-x}$)$_2$ZnSnSe$_4$ (p) /Cu2ZnSnSe$_4$ (p+) structure". Solar Energy **221** (2021) 314-322. https://doi.org/10.1016/J.SOLENER.2021.04.043

[37] S. Dubey, J.N. Sarvaiya, B. Seshadri," Temperature Dependent Photovoltaic (PV) Efficiency and Its Effect on PV Production in the World – A Review". Energy Procedia, **33** (2013) 311-321. https://doi.org/10.1016/J.EGYPRO.2013.05.072

[38] Mamta, K.K. Maurya, V.N. Singh," Enhancing the Performance of an Sb 2 Se 3 -Based Solar Cell by Dual Buffer Layer", 13, Layer. Sustainability **13** (2021) 12320. https://doi.org/10.3390/su132112320

[39] M. Lameirinhas, R.A., P. Correia V. Bernardo, C., N. Torres, J.P. *et al, al.* "Modelling the effect of defects and cracks in solar cells'. Scientific Reports **13** (2023) 12490. https://doi.org/10.1038/s41598-023-39769-0.

[40] F. Wang, S. Bai, W. Tress, A. Hagfeldt, F. Gao, "Defects engineering for high-performance perovskite solar cells". npj Flexible Electronics **2** (2018) 22. https://doi.org/10.1038/s41528-018-0035-z

[41] W. Zhao, W. Zhou, X. Miao, 7th IEEE International Conference on Nano/Micro Engineered and Molecular Systems (NEMS), (2012) 502-505. https://doi.org/10.1109/NEMS.2012.6196826.

[42] P. Ci, X. Tian, J. Kang, A.Salazar, K. Eriguchi, S.Warkander, K. Tang, J. Liu, Y. Chen, S. Tongay, W. Walukiewicz, J. Miao, O. Dubon, J. Wu, "Chemical trends of deep levels in van der Waals semiconductors". Nat. Commun. **11** (2020) 5373. https://doi.org/10.1038/s41467-020-19247-1

[43] W. Walukiewicz, "Amphoteric native defects in semiconductors". The Journal of Physical Chemistry Letters, **9**(14) (2018) 3878-3885. https://doi.org/10.1063/1.101174

[44] K. Cao, Y. Cheng, W. Zuo, B. Cai, Y. Wu, J. Zhu, Y. Zhu, H. Ning, Y. Shen, W. Shen, L. Liu, S. Chen, "Ionic compensation for defect reduction and enhanced performance of tin-based perovskite solar cells". J power sources **558** (2023) 232595. https://doi.org/10.1016/J.JPOWSOUR.2022.232595

[45] W.Walukiewicz, I. Rey-Stolle, G. Han, M. Jaquez, D. Broberg, W. Xie, M. Sherburne, N. Mathews, M. Asta, "Bistable Amphoteric Native Defect Model of Perovskite Photovoltaics". J. Phys Chem Lett. **9** (2018) 3878-3885. https://doi.org/10.1021/acs.jpclett.8b01446

[46] D. Ju, Y. Dang, Z. Zhu, H. Liu, C.C. Chueh, X. Li, L.Wang, X. Hu, A.K.Y. Jen, X. Tao, "Tunable Band Gap and Long Carrier Recombination Lifetime of Stable Mixed $CH_3NH_3Pb_xSn_{1-x}Br_3$ Single Crystals".Chem Mater. **30**(5) (2018) 1556–1565. https://doi.org/10.1021/acs.chemmater.7b04565

[47] M.C. Naylor, D. Tiwari, A. Sheppard, J. Laverock., S, Campbell, B. Ford, X. Xu, M.D.K. Jones, Y. Qu, P. Maiello, V. Barrioz, N.S. Beattie, N.A. Fox, D.J. Fermin, G. Zoppi, "Ex situ Ge-doping of CZTS nanocrystals and CZTSSe solar absorber films." Faraday Discussions **239** (2022) 70-84. https://doi.org/10.1039/d2fd00069e

[48] P. Punathil, E. Artegiani, S. Zanetti, L. Lozzi, V. Kumar, A. Romeo, "A simple method for Ge incorporation to enhance performance of low temperature and non- vacuum based CZTSSe solar cells", Sol Energy **236** (2022) 599-607. https://doi.org/10.1016/j.solener.2022.03.027

[49] C. Gao, Y. Sun, W. Yu, "Influence of Ge Incorporation from GeSe 2 Vapor on the Properties of Cu 2 ZnSn(S,Se) 4 Material and Solar Cells", Coatings **8**(9) (2018) 304. https://doi.org/10.3390/coatings8090304

[50] L.K. Ono, S. Liu (Frank), Y. Qi, "Reducing Detrimental Defects for High-Performance Metal Halide Perovskite Solar Cells". Angewandte Chemie International Edition **59**(17) (2019) 6676-6698, https://doi.org/10.1002/anie.201905521.

[51] M. He, C. Yan, J. Li, M.P. Suryawanshi, J. Kim, M.A. Green, X. Hao, "Kesterite Solar Cells: Insights into Current Strategies and Challenges", Adv. Sci. **8** (2021) 2004313. https://doi.org/10.1002%2Fadvs.202004313

[52] J. Kumar, P. Srivastava, M. Bag,. "Advanced Strategies to Tailor the Nucleation and Crystal Growth in Hybrid Halide Perovskite Thin Films". Solid Stat Chemis **10** (2022) 842924. https://doi.org/10.3389/fchem.2022.842924

[53] M.A. Islam, M.N.B. Alamgir, S.I. Chowdhury, S.M.B. Billah, "Lead-free organic inorganic halide perovskite solar cell with over 30% efficiency". Journal of Ovonic Research, **18**(3) (2022) 395–409. https://doi.org/10.15251/JOR.2022.183.395.

[54] K. Fatema, M.S. Arefin, "Enhancing the efficiency of Pb-based and Sn-based perovskite solar cell by applying different ETL and HTL using SCAPS-ID. Optical Materials **125** (2022) 112036. https://doi.org/10.1016/J.OPTMAT.2022.112036.

[55] S. Essig; C. Allebé, T. Remo; J.F. Geisz; M.A. Steiner; K. Horowitz; L. Barraud; J.S. Ward; M. Schnabel; A. Descoeudres; et al. "Raising the one-sun conversion efficiency of III–V/Si solar cells to 32.8% for two junctions and 35.9% for three junctions". Nat.Energy **2** (2017) 17144. https://doi.org/10.1038/nenergy.2017.144.

[56] M.M. Salah, A. Zekry; A. Shaker; M. Abouelatta; M. Mousa; A. Saeed, "Investigation of Electron Transport Material-Free Perovskite/CIGS Tandem Solar Cell". Energies **15** (2022) 6326. https://doi.org/10.3390/en15176326.

[57] A.D.K. Kenfack, N.M. Thantsha, M. Msimanga, "Simulation of Lead-Free Heterojunction CsGeI2Br/CsGeI3-Based Perovskite Solar Cell Using SCAPS-1D". Solar **3**(3) (2023) 458-472. https://doi.org/10.3390/SOLAR3030025.

[58] B. Saha, B.K. Mondal, S.K. Mostaque, M. Hossain, J. Hossain, "Numerical modeling of CuSbSe2-based dual-heterojunction thin film solar cell with CGS back surface layer". AIP Advances **13** (2023) 025255. https://doi.org/10.1063/5.0133889

[59] K.M. Katubi, N.S. Shiong, M.Z. Pakhuruddin, M.A. Alkhalayfeh, S.A. Abubaker, M.R. Al-Soeidat, "Over 35% efficiency of three absorber layers of perovskite solar cells using SCAPS 1-D". Optik **297** (2024) 171579. https://doi.org/10.1016/J.IJLEO.2023.171579.

[60] M.H. Azar; S. Aynehband; H. Abdollahi; H. Alimohammadi; N. Rajabi; S. Angizi; V. Kamraninejad; R. Teimouri; R. Mohammadpour; A. Simchi, "SCAPS Empowered Machine Learning Modelling of Perovskite Solar Cells: Predictive Design of Active Layer and Hole Transport Materials". Photonics **10** (2023) 271. https://doi.org/10.3390/photonics10030271

[61] M.M. Salah, A. Zekry, A. Shaker, M. Abouelatta, M. Mousa, A. Saeed, "Investigation of Electron Transport Material-Free Perovskite/CIGS Tandem Solar Cell". Energies **15**(17) (2022) 6326. https://doi.org/10.3390/EN15176326

[62] F. Baig, Y.H. Khattak, S. Ullah, B.M. Soucase, S. Beg, H. Ullah, Numerical analysis a guide to improve the efficiency of experimentally designed solar cell. Applied Physics A: Materials Science and Processing, **124**(7) (2018), 1–8. https://doi.org/10.1007/S00339-018-1877-X

[63] A. Houimi, S.Y. Gezgin, B. Mercimek, H.Ş. Kılıç, "Numerical analysis of CZTS/n-Si solar cells using SCAPS-1D. A comparative study between experimental and calculated outputs." Optical Materials **121** (2021) 111544. https://doi.org/10.1016/J.OPTMAT.2021.111544